AD-762 516

PROPAGATION OF MULTIWAVELENGTH LASER RADIATION THROUGH ATMOSPHERIC TURBULENCE

J. Richard Kerr

Oregon Graduate Center for Study and Research

Prepared for:

Advanced Research Projects Agency

15 April 1973

AD 762516

RADC-TR-73-164
Technical Report
April 1973

PROPAGATION OF MULTIWAVELENGTH LASER RADIATION
THROUGH ATMOSPHERIC TURBULENCE

Oregon Graduate Center for Study and Research

Sponsored by
Defense Advanced Research Projects Agency
ARPA Order No. 1279
Amend. 5

Approved for public release;
distribution unlimited.

The views and conclusions contained in this document are those of the authors and should not be interpreted as necessarily representing the official policies, either expressed or implied, of the Defense Advanced Research Projects Agency or the U. S. Government.

Rome Air Development Center
Air Force Systems Command
Griffiss Air Force Base, New York

UNCLASSIFIED

Security Classification

DOCUMENT CONTROL DATA - R & D

(Security classification of title, body of abstract and indexing annotation must be entered when the overall report is classified)

1. ORIGINATING ACTIVITY (Corporate author) Oregon Graduate Center for Study and Research Beaverton, Oregon 97005	2a. REPORT SECURITY CLASSIFICATION Unclassified
	2b. GROUP

3. REPORT TITLE

Propagation of Multiwavelength Laser Radiation through Atmospheric Turbulence

4. DESCRIPTIVE NOTES (Type of report and inclusive dates)

Quarterly report, December 15, 1972 - March 15, 1973

5. AUTHOR(S) (First name, middle initial, last name)

J. Richard Kerr

6. REPORT DATE April 15, 1973	7a. TOTAL NO. OF PAGES ~~33~~ 25	7b. NO. OF REFS 28
8a. CONTRACT OR GRANT NO. F30602-72-C-0470	9a. ORIGINATOR'S REPORT NUMBER(S) 1174-3	
b. PROJECT NO. 1279		
c. Program Code Number 3E20	9b. OTHER REPORT NO(S) (Any other numbers that may be assigned this report) RADC-TR-73-164	
d. ARPA Order Number 1279 Amend. 5		

10. DISTRIBUTION STATEMENT

Approved for public release, distribution unlimited.

11. SUPPLEMENTARY NOTES Monitored by: Raymond P. Urtz, Jr. RADC (OCSE), GAFB, N. Y. 13440	12. SPONSORING MILITARY ACTIVITY Advanced Research Projects Agency Washington, D. C. 20301

13. ABSTRACT

A tracking system for cancelling turbulence-induced beam wander has been operated and preliminary results are reported for mean irradiance and irradiance-fading on target. The experimental program now underway on wander-cancellation and finite-beam effects is described in detail.

New instrumental developments for the investigation of turbulence intermittency and its propagation effects are described, including a multiplexed field array of microthermal sensors for modeling the turbulence. The experimental program and new aspects of statistical data interpretation are discussed, with preliminary examples.

DD FORM 1 NOV 65 1473 (PAGE 1)

S/N 0101-807-6811

UNCLASSIFIED

Security Classification

A-31408

UNCLASSIFIED

Security Classification

14. KEY WORDS	LINK A		LINK B		LINK C	
	ROLE	WT	ROLE	WT	ROLE	WT
Propagation						
Turbulence						
Atmospheric Optics						
Scintillation						
10.6 Microns						

PROPAGATION OF MULTIWAVELENGTH LASER RADIATION
THROUGH ATMOSPHERIC TURBULENCE

J. Richard Kerr

Contractor: Oregon Graduate Center for Study and Research
Contract Number: F30602-72-C-0470
Effective Date of Contract: 15 June 1972
Contract Expiration Date: 15 June 1973
Amount of Contract: $75,682.00
Program Code Number: 3E20

Principal Investigator: Dr. J. Richard Kerr
Phone: 503 645-1121

Project Engineer: Mr. Raymond P. Urtz, Jr.
Phone: 315 330-3145

This research was supported by the Advanced Research Project Agency of the Department of Defense and was monitored by Raymond P. Urtz, Jr. RADC (OCSE), GAFB, NY 13441 under Contract F30602-72-C-0470.

PUBLICATION REVIEW

This technical report has been reviewed and is approved.

Raymond P. Urtz Jr.

RADC Project Engineer

Summary

A tracking system for cancelling turbulence-induced beam wander has been operated and preliminary results are reported for mean irradiance and irradiance-fading on target. The experimental program now underway on wander-cancellation and finite-beam effects is described in detail.

New instrumental developments for the investigation of turbulence intermittency and its propagation effects are described, including a multiplexed field array of microthermal sensors for modeling the turbulence. The experimental program and new aspects of statistical data interpretation are discussed, with preliminary examples.

TABLE OF CONTENTS

I. Introduction

Work in the period covered by this report includes (1) the cancellation of atmospherically-induced beam wander and the investigation of finite-beam effects on target-irradiance and fading, and (2) the investigation of the nature and propagation effects of the intermittency of turbulence. Preliminary wander-cancellation results are presented, and the ongoing experiments are described in detail. Illustrative data related to intermittency effects are also described, and progress on the theoretical framework, instrumentation, and significance of this problem are discussed.

II. Beam-Wander Cancellation and Finite-Beam Effects

The preceding report on this program[1] contains a detailed review of finite-beam wander, spread, and scintillation considerations. The goals of the present effort are (1) to demonstrate the cancellation of wander, utilizing a principle of reciprocity;[2] and (2) to quantitatively determine finite-beam wander and scintillation fading effects and relate these to theory, much of which has only recently been clarified.[1] We are primarily interested in the illumination of a point on a target plane, with the effects of tracking-out wander, and the statistics and spectra of the fading mechanisms as a function of the relevant parameters. This includes the improvement in both mean irradiance and degree of fading obtainable through tracking.

A. Instrumentation

As described in an earlier report,[3] the laser transmitter consists of a fast servoed tracking system with a 15 cm output aperture. The optics incorporate spatial filtering and are essentially diffraction-limited.

Quantitative results on linear and log fading and on mean irradiance at the target plane are obtained with the system shown in Figure 1. A silicon photodiode is dc-coupled through stable, low-noise amplifiers to

three processing circuits. The first of these provides an output proportional to the instantaneous logarithm of the input, while the second responds to the linear irradiance fluctuations. The third provides a signal proportional to the mean irradiance. All three outputs are recorded on an instrumentation tape recorder for statistical and spectral processing on a digital computer.

The target receiver is normally utilized as a point detector coincident with the center of a reflector or beacon which serves as a source for the transmitter tracking unit. When this tracking source is large (e.g., several cm), the small photodetector is suspended at its center (Figure 2a). When it is small, a 45° mirror with a center hole is utilized (Figure 2b). These sources are discussed further in a later section. In general, beamsplitting mirrors are avoided because scattering off of dust and imperfections causes the detector to respond to reflector or beacon energy. There is also a provision for utilizing finite receiver optics in order to spatially-smooth the scintillation effects.

The receiver, recording, and tracking source units are mounted in a mobile van which may be used at various distances from the transmitter (typically on the order of 1 km). A microthermal probe system is used for the non-optical measurement of turbulence strength, or equivalently, the coherence parameter ρ_o (see Ref. 1).

Data processing is performed on a DEC/PDP-11 computer, which is programmed to determine (linear and log) probability distributions and variances, and FFT power spectra.

B. Preliminary Results

The initial operation of the tracker electronics is shown qualitatively in Figure 3. The oscillograph represents the difference signal between two opposing quadrants in the tracking photodetector, and in the open-loop case indicates the apparent angular wandering of the target. When the servo-controlled galvanometric scanner mirrors are activated, this signal is substantially eliminated; the remaining high-frequency noise

is due to scintillation and tracker-response as limited by natural frequencies of the galvanometers. The signal of Figure 3a shows the characteristically low frequencies (≈ 1 Hz) involved in beam wander (or image dancing) phenomena.

The effect of tracking on the (point) irradiance at the target is shown in Figure 4. The mean irradiance is increased approximately 3 dB and is stabilized against long-term drift. The ratio of the transmitter diameter (b) to the coherence radius ρ_o was not determined; according to Figure 19 of Ref. 1, the improvement in mean irradiance can be two or three times this amount when b/ρ_o is properly controlled, as will be done as part of this investigation.

The fluctuations or fading shown in Figure 4 are due to wander and scintillations, although low-pass filtering has removed some of the latter in this figure. In order to remove scintillations from the determination of wander-fading, the log amplitude variances with and without tracking have been determined as a function of low-pass cutoff frequencies. The results are given in Table I, and show that, although scintillations strongly predominated, the fading related to wander is indeed drastically reduced: for a cutoff frequency of 1 Hz, which leaves negligible scintillation components but much of the wander (Figure 3), the reduction in variance due to tracking is a factor of nearly 20. On the other hand, when scintillation components up to 1 kHz are included, the reduction in total fading is nominal. In the quantitative experiments in this investigation, it will be essential to monitor and control b/ρ_o so that the results can be related to theory (Figure 20 of Ref. 1) and a substantial reduction of total fading demonstrated.

Table I. Log amplitude variance vs cutoff frequency.

Bandwidth of Photocurrent	$\sigma^2_{\text{no track}}$	σ^2_{track}	$\dfrac{\sigma^2_{\text{track}}}{\sigma^2_{\text{no track}}}$
0-1 kHz	0.53	0.40	0.75
0-10 Hz	0.0047	0.00085	0.18
0-1 Hz	0.0020	0.00011	0.055

The power spectra of irradiance fluctuations, with and without tracking, are shown in Figure 5, and again indicate that the significant wander components are below a few Hz. The computer program is being modified to expand the low-frequency scale of such a plot.

The highly preliminary and nonoptimum results given above were obtained with the use of a 7 cm retroreflector for a target beacon source. As discussed below, this choice can lead to poor results and has been superseded. The preliminary experiments also pointed out improvements needed in the tracking transmitter mechanical arrangement and electronics; these are currently being implemented.

C. Experimental Plan

In order to fully investigate the potential of wander-tracking and transmitter-aperture control to improve average illumination and fading characteristics, we will conduct experiments under a wide range of parameters, employing several techniques for interpreting the data. Ideally, this will include all of the following elements:

1) Raw data

The basic data will consist of

a) Recording of log and linear signals at the target

b) Microthermal determination of C_n^2 or ρ_o

c) Recording of microthermal fluctuations $\Delta T(t)$

d) Record or vectorscope picture of (x, y) scanner input signals in tracker servo

e) Record of general meteorological conditions, etc.

2) Variables and Parameters

a) Open/closed loop servo (i.e., no-track/track condition)

b) Size of receiver at target

c) Transmitter size (b)

d) C_n^2 or ρ_o

e) Low-pass cutoff frequency of signal at target

f) Transmitter focus conditions

g) Lateral position relative to centroid of target illumination

h) Range (L)

3) Processing

a) Spectrum of ΔT, to monitor presence of inertial subrange[4] and determine inner scale (ℓ_o)

b) Mean target irradiance $\bar{I}$

c) Log amplitude variance at target (σ^2)

d) Power spectrum of signal at target

e) Probability distribution of linear and/or log signal at target

4) Interpretation

The major independent parameter in interpreting the data is the ratio b/ρ_o (see Ref. 1), and this ratio is the appropriate abscissa in most data plots. The detailed phenomena to be investigated are as follows:

a) Effect of tracking and transmitter size on mean irradiance.

The applicable theory for comparison with experimental results is represented by Figs. 18,

19 in Ref. 1, and includes the prediction of a substantial increase in $\bar{I}$, using wander-cancellation and an appropriately-chosen transmitter aperture.

b) Effect of tracking and transmitter size on fading of target signal due to wander and scintillation. The applicable theory is related to Fig. 20 of Ref. 1. In addition to the elimination of fading due to wander, the theory[5] predicts a substantial reduction in scintillation, for a carefully adjusted transmitter with the proper aperture size. This has not been quantitatively investigated in the past, since wander-cancellation is required. To aid in these experiments, the effects of wander and scintillation may be mutually separated by reducing the latter through variable-receiver-aperture spatial-smoothing, or variable low-pass electronic smoothing. Equivalently, the power spectrum of fading, including appropriate resolution at a few Hz and below, may be utilized.

c) Probability distribution and power spectrum of wander-fading.
The theoretical power spectrum may be deduced from image-dancing theory,[7] and the statistics are predicted in the recent literature.[8,9]

d) Mean-square wander angle (obtained from item 1-d).
The applicable theory is related to Fig. 21 and Eqs. (24, 25, 28, 30) of Ref. 1.

e) Mean-square instantaneous spread angle, as deduced from mean irradiance with wander tracked out (item 4-a).

It is our plan to cover most or all of these items. In addition, we will return to the question of deliberate angular-beam-dither as discussed in Ref. 1. Finally, certain theoretical details remain to be clarified, as discussed in that reference and below.

D. Beacon/Reflector Considerations

The subject of this investigation is the illumination of a point on a (possibly-resolvable) target, and the development of sophisticated, image-processing trackers is beyond the scope of the effort: the results obtained through the use of a cooperative reflector or beacon are valid and will be immediately applicable to such systems.

The results described in section B were obtained with a resolvable (7 cm) retroreflector at the target. We now consider this to be a sub-optimum choice of tracking source, for the following interrelated reasons:

1) Scintillations within the retro cross-section constitute a spurious input to the tracker, in that they contribute to the apparent centroid motion of the target.

2) Elements of beam wander which are resolvable within the retro cross-section will have an apparent motion which is two times that observed for larger, overall beam components. This is a consequence of the lateral displacement of rays in a corner cube.

3) The atmospheric bending of rays may not be perfectly correlated over the entire retro cross-section, so that the tracker is not truly optimizing the wander-cancellation at a central point.

4) The coherent illumination of a resolvable reflector can lead to gross tracker errors due to the phenomenon of "angular scintillation."[10-12] The implications of reciprocity with relation to this effect are not fully understood, but it is clearly desirable to avoid the phenomenon.

In order to eliminate these problems, we can utilize a small retro. However, the resulting SNR in the simple tracker is then less than ideal. Consequently, we are now employing a small beacon-laser[13] at the target, which does not invalidate the reciprocity considerations underlying this work. In order to utilize a point detector for target irradiance measurements, the beacon can be enlarged (Fig. 2a) to a size comparable to the transmitter resolution scale ($\approx$ 1 cm) and defocused sufficiently to eliminate pointing problems.

E. Scintillation with Large Apertures

As discussed in Ref. 1, the application of reciprocity theory to Fried's analysis of "atmospheric modulation noise" (coherent fading) in an optical heterodyne receiver[14] suggests that the scintillation of target irradiance will grow indefinitely with increasing transmitter aperture size ($b \gg \rho_o$). We are convinced that this is not the case, which indicates an unidentified breakdown[16] in the conditions for validity of this particular analysis at large b/ρ_o. To support this contention, we cite the following points:

1) The experiments reported in Ref. 6 indicate that the scintillations for $b \gg \rho_o$ approach those for a plane-wave source in saturation.[17] This will be further verified on the present program.
2) A simple consideration of phase-independent oscillators of identical frequency,[18] representing the discrete ρ_o areas on the large transmitter (or reciprocal heterodyne-receiver) aperture, leads to a saturation of the target (or heterodyne) signal variance vs b.
3) In some recent Russian theoretical work,[19] which included the multiple scattering regime, it was shown that scintillations will saturate (vs b) for large values of the phase structure function $D_\phi(b)$.

In addition, the spatial scale of the scintillation patches is predicted to be the transmitter diffraction scale, as we surmised in Ref. 6.

F. Cancellation of Beam Wander for Uplink

In the preceding report (Ref. 1), it was stated that the cancellation of beam wander, with the attendant advantages in mean illumination and fading, was of no value in the far field of the transmitter. This statement presupposes a constant level of turbulence between transmitter and target (horizontal path), and must be modified for the vertical case. In particular, if the turbulence is confined to the near field of the transmitter on an uplink, we may expect advantages similar to those for the horizontal case, with similar analytical predictions once ρ_o is determined from the reciprocal downlink. This may be seen from a consideration of this reciprocal downlink: since the phase structure function $D_\phi(b)$ is substantially equal to the wave structure function $D(b)$, the conditions for ignoring amplitude scintillation effects are satisfied. As pointed out by Brown,[18] wander-cancellation may be especially valuable in an uplink, due to the large turbulence scales which may be encountered and which lead to geometrical beam-bending effects.

III. Turbulence Intermittency

The macroscopic intermittency of atmospheric turbulence, which is observed under many conditions, gives rise to large fluctuations in scintillations and other propagation effects, and leads to large data-spreads in quantitative experiments. The use of very-long averaging times to eliminate these effects obviously masks short-term peaks in the scintillation level, and hence masks deep fading. Thus, there is a strong motivation to understand the statistics of the intermittency and its propagation effects; this has been further strengthened by recent interest in fast, single-shot optical systems, e.g., using millisecond pulses or imaging, in which the atmosphere is effectively frozen so that short-term statistics apply.

We define intermittent turbulence[1] as being indicated by random microthermal fluctuations $\Delta T(t)$ which have a random modulating or miltiplicative-envelope function whose characteristic frequencies are significantly lower than the lowest-frequency components of interest in the basic fluctuations. This lower limitation on "interesting" frequencies relates to the outer scale of the Kolmogorov spectrum, or to the lowest spatial turbulence scales within the optical/IR scintillation filter functions.

A typical microthermal signal showing intermittent turbulence is given in Figure 6. The interesting measurement times are on the order of the envelope fluctuation times. A period of high turbulence may appear for e.g. 5 seconds at a measurement point; if the wind speed* is 2 m/sec, the turbulence region has a spatial extent (along the wind) of 10 m. Although this region may be warmer and hence carry <u>additive</u> low frequencies in $\Delta T(t)$, these additive components do not affect scintillation and are not of interest; the multiplicative low frequencies simply create narrow sidebands around each of the higher-frequency components of $\Delta T(t)$, and do not noticeably affect the autocorrelation or power spectrum.

The degree of meteorological understanding of macroscale turbulence intermittency is poor, so that mostly empirical means are necessary for modeling the turbulence statistics. With the use of these models, and an understanding of the relationship to short-term propagation statistics, it will be possible to generate appropriate data for inputs to computer codes which simulate propagation effects.

----

* The actual mean wind speed for the microthermal data of Figs. 6, 9-12 was 1.3 m/sec.

A. Instrumental Developments

The basic field site constitutes a one-mile path over uniform terrain, with coincident, simultaneous point-source laser beams at 4880 Å and 10.6 μ wavelengths, and wide-dynamic-range receiver electronics. In addition, a microthermal probe system permits the recording of microthermal variations $\Delta T(t)$. These facilities have been extensively described in previous reports.

We are now replicating the microthermal probes, in order to investigate the spatial-correlation scales of the short-term turbulence strength (C_n^2). For later use, we are designing a 10-probe-pair array, with common cabling and multiplexed recording of short-term C_n^2 from each pair. The individual pairs will be movable and can be lined up in an "L" configuration parallel and perpendicular to the wind direction.

The basic new microthermal system is shown schematically in Figure 7a. The probe pair is differentially ac-driven with a 100 kHz oscillator, and the difference in probe resistances generates a net ac input to an amplifier. The output is synchronously demodulated and low-pass filtered to remove the carrier, resulting in a signal proportional to $\Delta T(t)$.

The signal is then squared, resulting in an output proportional to $\Delta T^2(t)$, and it is also used with a voltage-controlled current source and capacitor to generate long-term-average signal $\overline{\Delta T}$, which represents the static and slowly-drifting imbalance of the probe pair. This latter voltage, which may typically have a 1 minute time constant, is utilized with an analog multiplier in a feedback loop, to keep the probe pair in long-term balance.

Multiplexing of a number of probe pairs, with common cabling, is then accomplished as shown in Figure 7b. A synchronous multiplexing switch commutates the probe pair being demodulated, as well as the corresponding (stored) $\overline{\Delta T}$ signal for balance. The $\Delta T^2(t)$ signal is averaged (integrated) over a single time window (τ), and is then "dumped" to make ready for the next probe pair. This multiplexed sample-mean is then

recorded on an instrumentation recorder, along with the multiplexing signal.

The demultiplexing process is shown conceptually in Figure 8. The voltages on each capacitor represent a sample-hold, short-term average of $\Delta T^2(t)$ (i.e., they represent $C_n^2(t)$) for the corresponding probe-pair. These signals may be further averaged to give long term values of C_n^2, or they may be cross-correlated, as in the present application. In practice, the data-processing step shown in Figure 8 will be accomplished on a digital computer.

If the number of probe pairs is N, the complete commutation period T_M is on the order of $N\tau$. The limitations on the system are that (1) T_M must be shorter than the variation-time-scales of interest in $C_n^2(t)$, and (2) the individual time window $\tau = T_M/N$ must be somewhat larger than the inverse recorder bandwidth. Referring to Figure 6, which is a typical trace of intermittent turbulence, the decorrelation times in $C_n^2(t)$ are on the order of a few seconds; if we choose $T_M = 0.1$ sec and $N = 10$, we have a recorder-bandwidth requirement of only a few hundred Hz. The final averaging, for noise-free correlation results, can be continued for as long as the data record permits; the effective averaging period in real time T will be on the order to T/N.

B. Computer Data Processing

We will utilize a DEC/PDP-11 digital computer for several data processing functions, whose applications will be discussed in a later section. These functions are currently operational.

1) Determination of the probability distributions of thermal fluctuations (and scintillations), and their variances. A number of successive (1 msec) signal-samples can be averaged, to give composite samples; this corresponds to variable-low-pass filtering or averaging of the raw signal, and can influence the probability distribution in important ways, as discussed below.

2) Direct determination of higher-order moments, vs averaging time.

3) Determination of the variance of a sequence of finite-observation-time variances (variance noise[20]), as a function of observation (averaging) time. In this case, the individual samples of raw data are not averaged, but the observation time or number of samples used in calculating each initial variance is varied, and then the "variance of variances" is calculated. This corresponds to squaring before averaging, and the technique can be applied to higher moments also.

4) Determination of the power spectrum of $\Delta T(t)$ and $\Delta T^2(t)$, and scintillations, including the low frequencies (<1 Hz) associated with the envelope of intermittencies.

C. Basic Field Data

The pertinent basic field data are as follows.

1) To model the intermittent turbulent field:
Record the multiplexed $\overline{\Delta T^2}\Big|_\tau$, where the averaging time τ is much less than one second, for probe-pairs at a number of points separated along lines parallel and perpendicular to the wind direction. Simultaneously, measure and record $\Delta T(t)$ (single-probe, no averaging) at one point.

2) To relate the optical/IR scintillation quantities to the intermittent turbulence:
Simultaneously with #1 above, record the log amplitude fluctuations $\ell(t)$ at the two wavelengths.

In all cases, conditions with grossly varying turbulence parameters, such as days with broken clouds, will be avoided, since this does not constitute the type of intermittency of interest. For each run, recordings will be made (or interpreted) for as long as possible before diurnal variations are dominant. The runs should be made under a number of different turbulence conditions, and also for a few similar conditions in order to check the repeatability of results.

D. Interpretation of Data; Statistical Descriptions

We are dealing basically with two random variables: the log amplitude optical or infrared variance $\ell(t)$, and the microthermal fluctuations $\Delta T(t)$. The former variable is normally distributed, and the latter is approximately (bilateral) log normally distributed.[21] Also, in the presence of intermittency, the latter has the nature of a multiplicative or envelope-modulated random variable, as described above. In the non-saturated scintillation regime, $\ell(t)$ is linearly related to ΔT^2 through a weighted integral over the propagation path. Our goals are to understand the statistical nature of intermittency and its relationship to averaging times, scintillation statistics, and experimental data-spread.

The determination of the statistical properties of the microthermal fluctuations will hopefully lead to a meaningful empirical model for intermittent turbulence near the ground. In Figure 9, we show the probability distribution of log $|\Delta T(t)|$, for various averaging times ranging from virtually zero averaging (1 msec) to 256 msec. The log normal character of the variable is evident within certain probability limits, especially for 64 msec averaging. In those determinations, the total observation time was 10 minutes.

As the averaging time increases, corresponding to a decreased low-pass-filter cutoff frequency, we expect the intermittency to affect the statistics, because the envelope of ΔT will show up as a slowly-varying mean or additive low frequency in $|\Delta T|$. In fact, for a sufficient averaging time, we expect the statistics of $\overline{|\Delta T|} \sim C_n(t)$ to become gaussian. In

Figure 10, we show the theoretical fourth moment (calculated from lower moments), for a log normal distribution,[22] divided by the actual fourth moment, as a function of averaging time. The crossover or agreement with log normality occurs at approximately 0.1 sec averaging. In figure 11, we show the same ratio for a normal distribution, and note the approach to unity at approximately 20 seconds averaging. As suggested by Figure 6, this constitutes sufficient averaging of the intermittency scale. The total observation time in these determinations was again 10 minutes.

In Figure 11, we note an irregularity in the curve for averaging times of a few seconds. This corresponds to the characteristic time scale of the intermittency. Another statistical description is the spread in variances, as a function of the observation time for each variance. The "variance of variances", normalized by the mean variance in each case, is shown vs observation time in Figure 12. We again observe an irregularity or noisiness for time scales of a few seconds.

The examples given above, although very preliminary, show the types of empirical statistics which can be used to model the intermittent turbulence, and we discuss these aspects in more detail below.

Collins has suggested[23] that intermittent turbulence cannot be rigorously described by a Fourier (Stieljes) spectrum. The difficulty may be that the establishment of low-frequency sidebands on each basic component of the microthermal spectrum violates the condition of "orthogonal increments".[24] This may in turn explain the formal breakdown of certain theoretical treatments, such as those for averaging time effects.[25]

We now review the specific statistical problems which will be addressed in this investigation:

1) Averaging time considerations

In the absence of intermittency, treatments of averaging-time effects (such as the convergence of variance samples to their true mean)[25] are influenced by the non-gaussian nature of $\Delta T(t)$, although they will apply to measurements of $\ell(t)$ or log amplitude scintillation variance. In the

presence of intermittency, the treatments apparently break down altogether, due to the multiplicative nature of the phenomenon. The resultant microthermal fluctuations exhibit apparent (i.e., short-term) nonstationarity, but the intermittency does not show up in the observed power spectrum or autocorrelation function of $\Delta T(t)$, although it will show in $|\Delta T(t)|$ or $\Delta T^2(t)$. Formally, the Fourier representation may be inapplicable, as discussed above, and averaging time considerations may be largely confined to empirical descriptions.

2) Measurement-sampling statistics (linear regression, correlation, confidence intervals)

We are interested in investigating experimental data-spread, including the influence of intermittency. In the absence of intermittency, and for moderate averaging times, we expect C_n^2 samples to be normally distributed, as will the σ^2 samples. The application of standard statistical methods[26] to relate empirical values of C_n^2 and σ^2 is straightforward. In the presence of intermittency, and for interesting averaging times, C_n^2 samples will not be normally distributed (Figure 11), and the same may be true of σ^2. Hence, the standard methods--such as the chi squared test--require reformulation.

3) Application of theoretical relationships between C_n^2 and σ^2

In the nonsaturation regime, which normally applies at 10 μ wavelengths if not in the visible, the two measure-

ments are linearly related by the physics of the problem:

$$\sigma^2 = \int_0^L C_n^{\,2}(z)\, f(z)\, dz \quad , \qquad (1)$$

where z is the propagation-path variable and L the pathlength. In the absence of intermittency, $C_n^{\,2}$ and σ^2 are normally distributed, and the above relationship should be usable to <u>predict</u> the statistics of σ^2 samples (such as their spread or variance vs averaging time) from statistics of $C_n^{\,2}$ samples. It is clear that the spatial correlation of $C_n^{\,2}$ is involved, and this motivates development of the microprobe array discussed above. In the presence of intermittency, the samples are not normally distributed, and an analytical model for $C_n^{\,2}$ would be required to predict complete σ^2 statistics. This may be intractable, but we can nevertheless recognize the relationship[27]

$$\left\langle (\sigma^2)^2 \right\rangle \sim \left\langle C_n^{\,2}(z_1)\, C_n^{\,2}(z_2) \right\rangle , \qquad (2)$$

where the quantity on the RHS will be investigated with the microprobe array. Higher moments can be similarly treated. Hopefully, σ^2 statistics can be sufficiently well determined to predict the percentage and mean length of time that the short-term variance is above any given level, which relates to "deep fades," and to fast systems (frozen atmosphere).

Since the necessary data will be on hand, we will also determine the spectral covariance[28] or cross-wavelength-correlation of scintillations.

E. Other Aspects

Although the present investigation is limited to scintillation, the intermittency phenomenon will have important effects on other propagation parameters, such as coherence and image resolution. An investigation of these topics will be deferred for the present.

Finally, it is apparent that characterization of the intermittency is also desirable at higher altitudes.

IV. Publications and Presentations

During the period covered in this report, the following papers have been published or presented:

1. J. R. Kerr and J. R. Dunphy, "Experimental Effects of Finite Transmitter Apertures on Scintillations," J. Opt. Soc. Am. 63, January 1973, pp. 1-8.
2. J. R. Dunphy and J. R. Kerr, "Scintillation Measurements for Large Integrated-Path Turbulence," Spring Meeting OSA, March 13-16, 1973, Denver, Colorado.

The latter paper has been submitted for publication in J. Opt. Soc. Am.

V. References

1. "Propagation of Multiwavelength Laser Radiation through Atmospheric Turbulence," RADC-TR-73-54, January 1973, Rome Air Development Center.
2. D. L. Fried and H. T. Yura, J. Opt. Soc. Am. 62, 600 (1972).
3. "Propagation of Multiwavelength Laser Radiation through Atmospheric Turbulence," RADC-TR-72-288, October 1972, Rome Air Development Center.
4. J. Richard Kerr, J. Opt. Soc. Am. 62, 1040 (1972).
5. J. R. Kerr and R. Eiss, J. Opt. Soc. Am. 62, 682 (1972).

6. J. R. Kerr and J. R. Dunphy, J. Opt. Soc. Am. 63, 1 (1973).

7. V. I. Tatarski, Propagation of Waves in a Turbulent Atmosphere, Nauka, Moscow, 1967.

8. D. L. Fried, Appl. Opt. 12, 422 (1973).

9. P. J. Titterton, Appl. Opt. 12, 423 (1973).

10. M. I. Skolnick, Introduction to Radar Systems, McGraw-Hill Book Co., New York, 1962.

11. J. P. Hansen and S. Madhu, Appl. Optics 11, 233 (1972).

12. W. Bridges, Hughes Research Laboratories, Malibu, Calif., private communication.

13. D. L. Fried, Optical Science Consultants, Inc., Yorba Linda, Calif., private communication.

14. D. L. Fried, J. Quantum Electr. QE-3, 213 (1967).

15. D. L. Fried, "Performance of a Fast-Tracking Laser Antenna," Spring Meeting, Opt. Soc. Am., April 11-13, 1972, New York, N.Y., Paper WE-18.

16. P. J. Titterton, Sylvania Electronic Systems, Inc., Mt. View, Calif., private communication.

17. R. S. Lawrence and J. W. Strohbehn, Proc. IEEE 58, 1523 (1970).

18. W. P. Brown, Jr., "Research in Interaction of Coherent Light with Solids and with Turbulent Atmospheres," Research Report, Hughes Research Laboratories, Malibu, Calif., May 1972.

19. K. S. Gochelashviiy, "Focused Irradiance Fluctuations in a Turbulent Medium," preprint, P.N. Lebedev Physical Institute, Academy of Sciences of the USSR, Moscow, 1971.

20. W. E. Purcell, J. Appl. Phys. 43, 2890 (1972).

21. R. W. Stewart, J. R. Wilson, and R. W. Burling, J. Fluid Mech. 41, 141 (1970).

22. J. Aitchison and J. A. C. Brown, The Log Normal Distribution, Cambridge University Press, London, 1966.

23. S. Collins, Ohio State University, private communication.

24. J. L. Lumley and H. A. Panofsky, The Structure of Atmospheric Turbulence, John Wiley and Sons, Inc., New York, 1964.

25. P. L. Hunt and S. A. Collins, Jr., "Averaging Times for Atmospherically Degraded Light Beam Measurements," Paper W0-18, Optical Society of America Annual Meeting, October 17-20, 1972, San Francisco, California.

26. J. S. Bendat and A. G. Piersol, Measurement and Analysis of Random Data, Wiley and Sons, New York, 1966.

27. W. P. Brown, Jr., private communication

28. D. L. Fried, Appl. Opt. 10, 721 (1971).

VI. Figures

1. Simplified schematic diagram of receiver for measurement of irradiance characteristics at target plane.
2. Mechanical arrangements for tracking source and detector of Fig. 1.
   a) Large tracking source
   b) Small tracking source
3. Signal corresponding to angular image position in tracker. Horizontal scale: 2 sec/division.
   a) Without tracking servo
   b) With tracking servo
4. Irradiance at target with and without tracking of atmospheric beam-wander. High frequency scintillations have been filtered out.
5. Power spectrum of irradiance fluctuations at target, with and without tracking.
6. Microthermal fluctuations $\Delta T(t)$ showing intermittent envelope. Time scale: 5 sec/division.
7. Microthermal probe array system.
   a) Basic system
   b) Multiplexing system
8. Conceptual diagram of demultiplexing process corresponding to Fig. 7.
9. Cumulative probability function for $\log |\Delta T|$.
   a) Averaging times of 1, 16, and 256 milliseconds.
   b) Averaging time of 64 milliseconds.

10. Ratio of theoretical fourth moment for log normal distribution to measured fourth moment of $|\Delta T|$, as a function of averaging time.

11. Same as figure 10, for normal probability distribution.

12. Variance of a set of empirical variances of ΔT, as a function of observation time for each empirical variance. The ordinate is normalized by the mean variance for each averaging time.

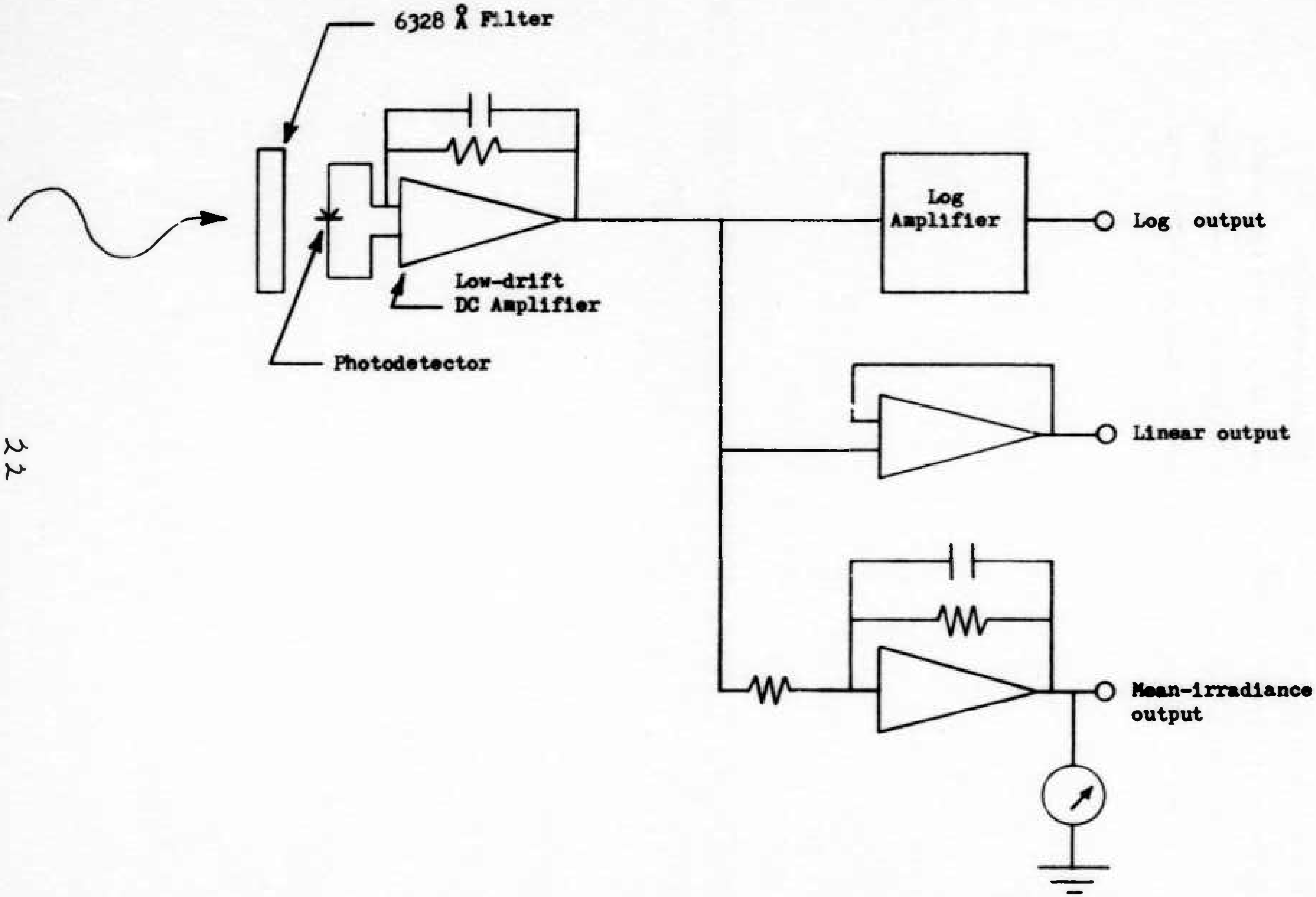

6328 Å Filter
Low-drift
DC Amplifier
Photodetector
Log
Amplifier
Log output
Linear output
Mean-irradiance
output

FIGURE 1

a)

b)

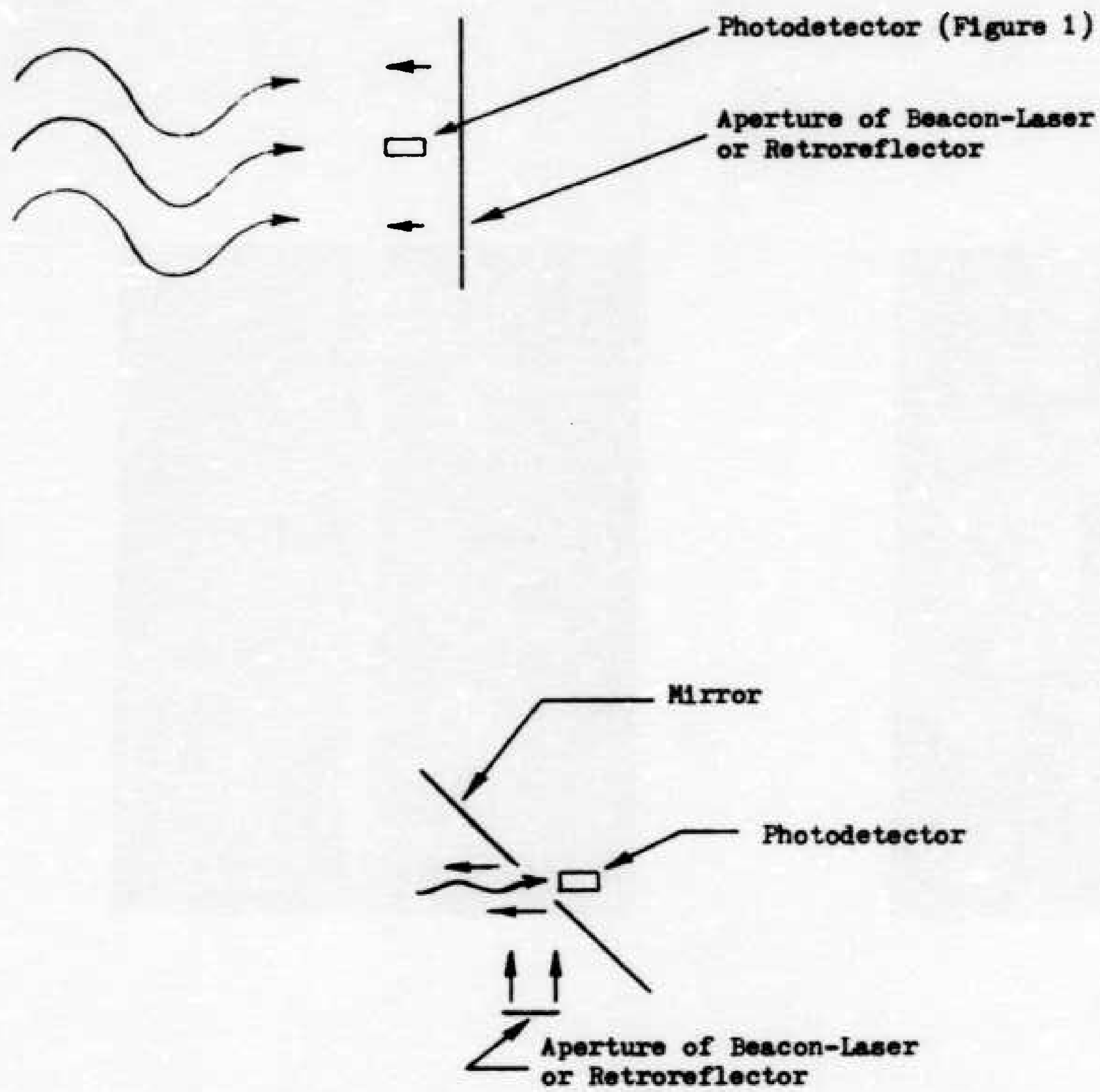
Photodetector (Figure 1)
Aperture of Beacon-Laser or Retroreflector
Mirror
Photodetector
Aperture of Beacon-Laser or Retroreflector

FIGURE 2

a)

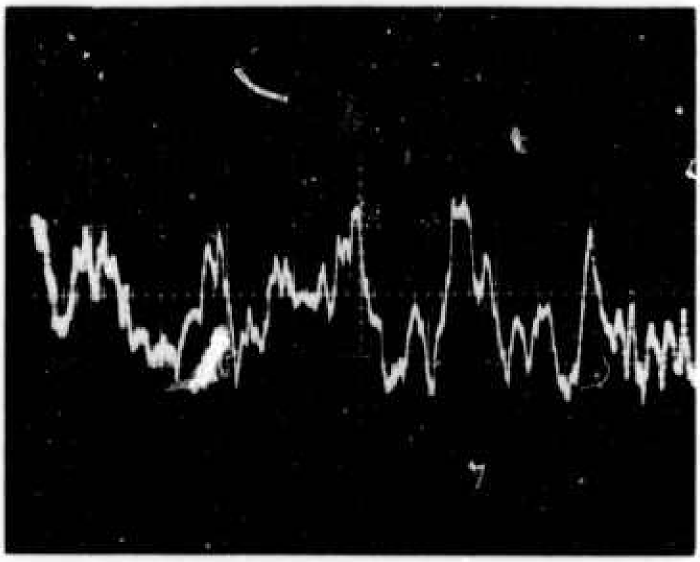

b)

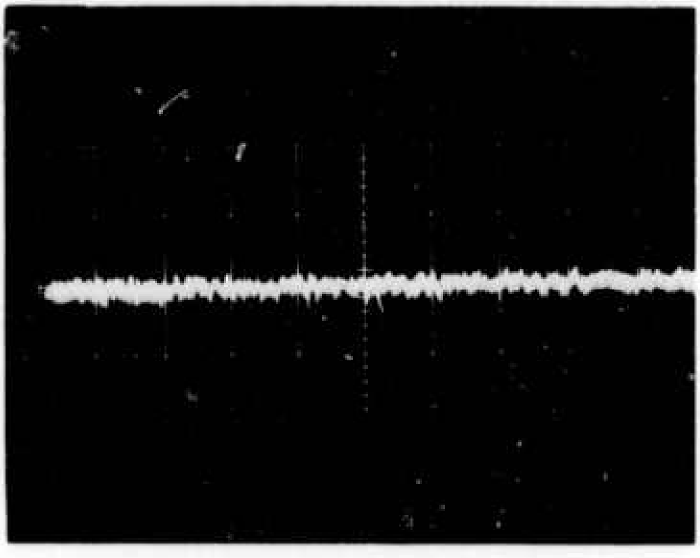

FIGURE 3

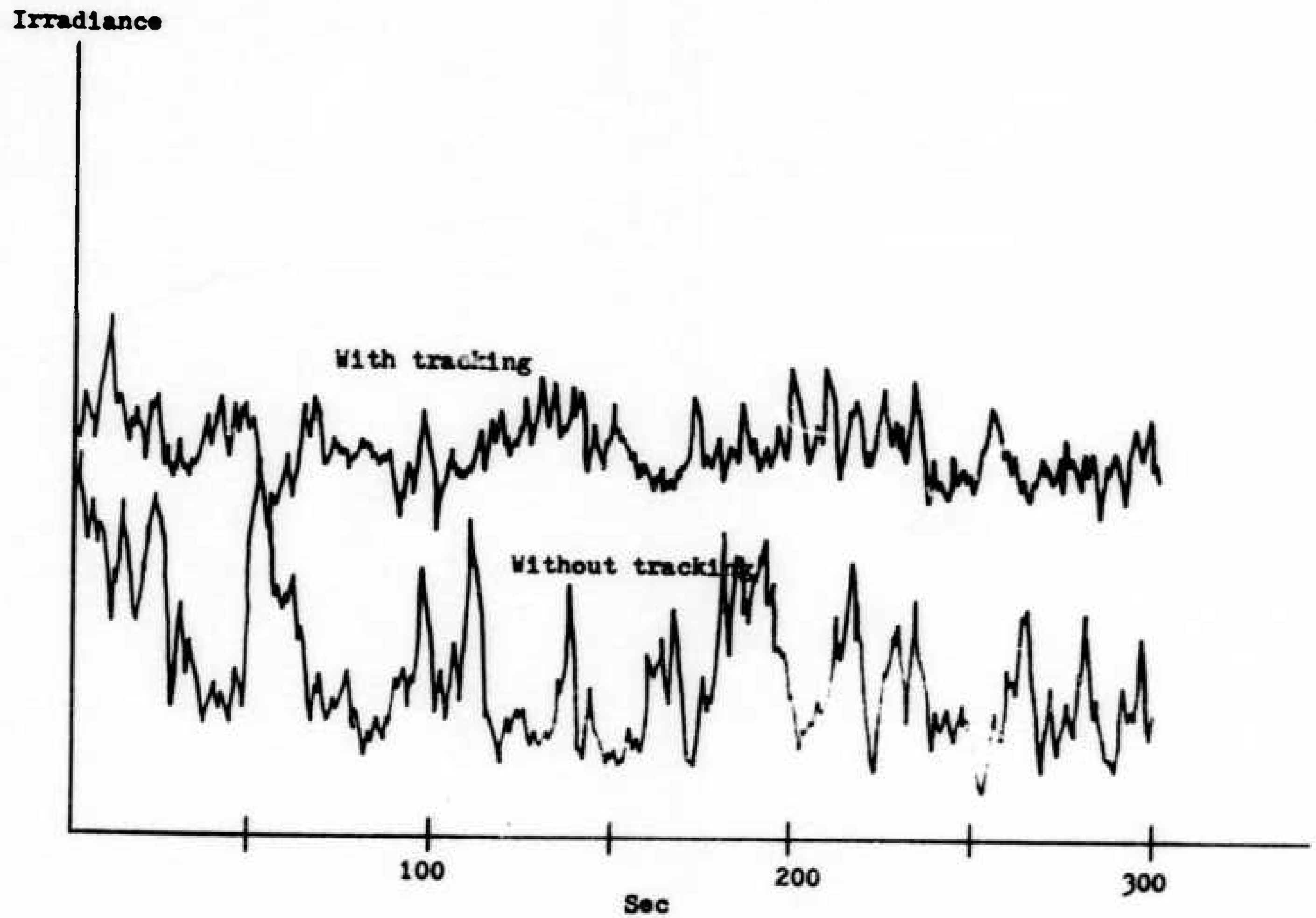

FIGURE 4

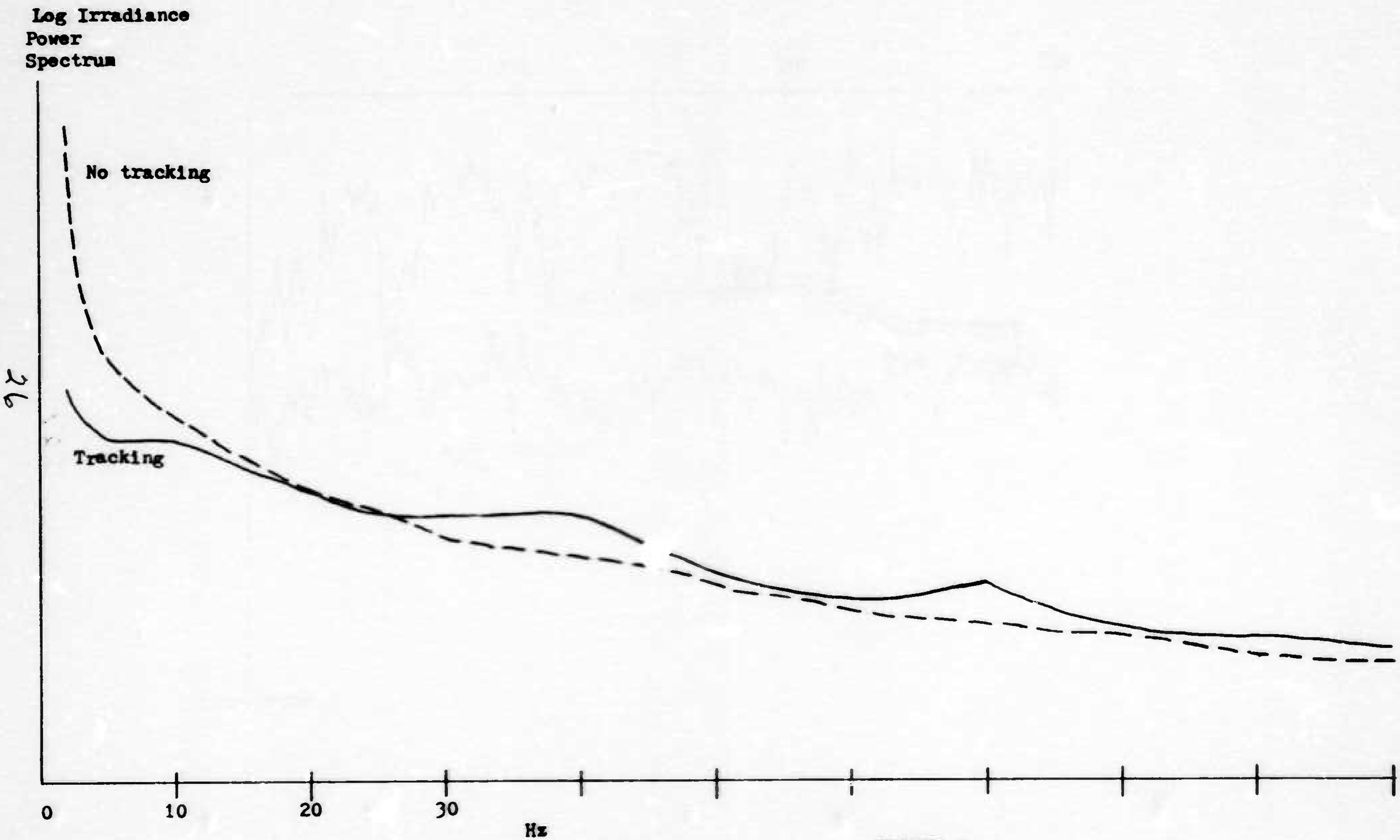
Log Irradiance
Power
Spectrum
No tracking
Tracking
0
10
20
30
Hz

FIGURE 5

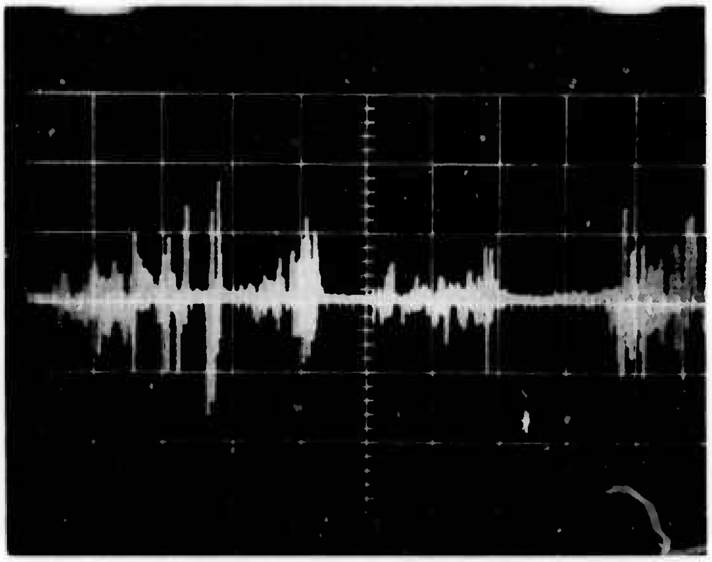

FIGURE 6

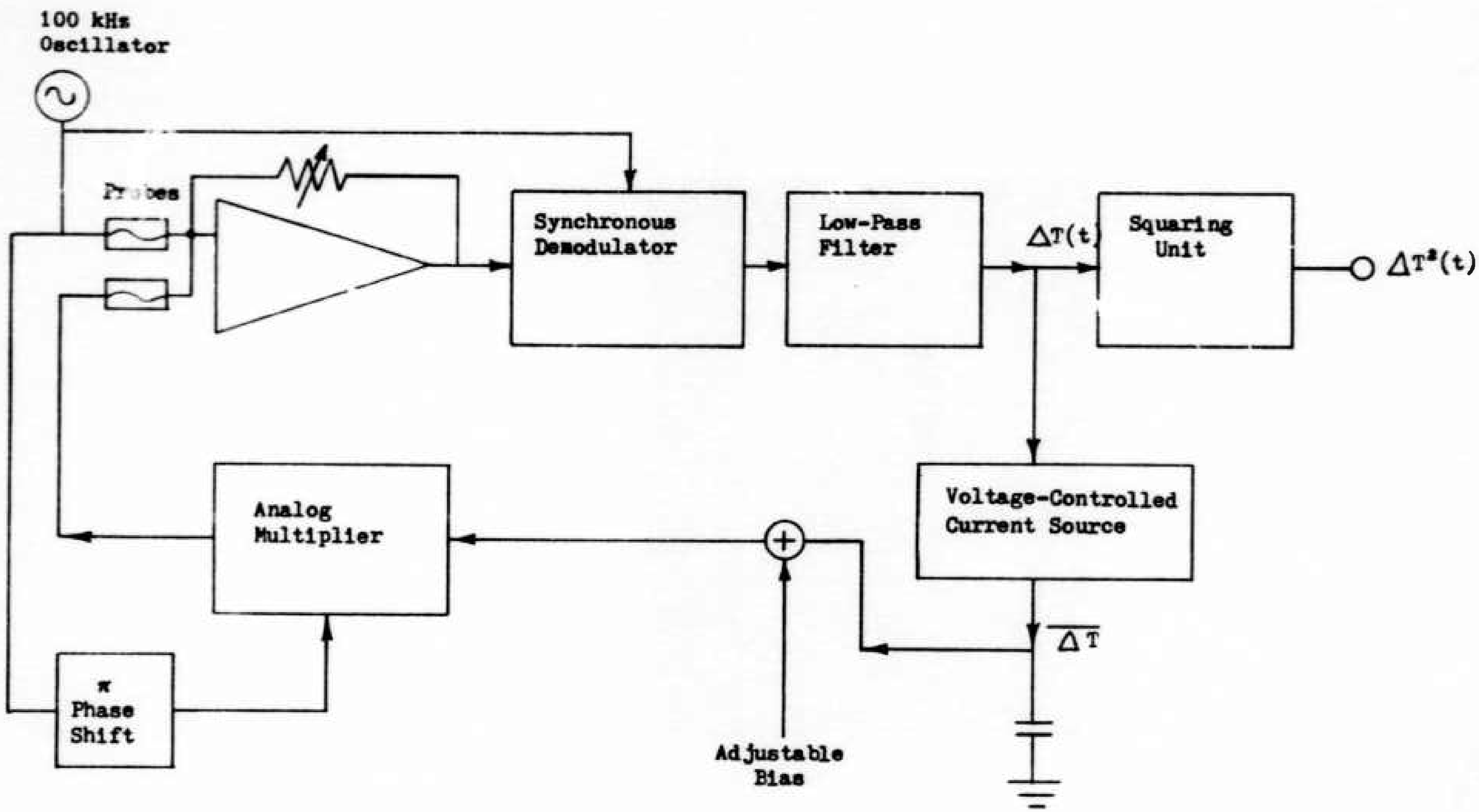
100 kHz
Oscillator
Probes
Synchronous
Demodulator
Low-Pass
Filter
ΔT(t)
Squaring
Unit
ΔT²(t)
Voltage-Controlled
Current Source
ΔT
Analog
Multiplier
π
Phase
Shift
Adjustable
Bias

FIGURE 7a

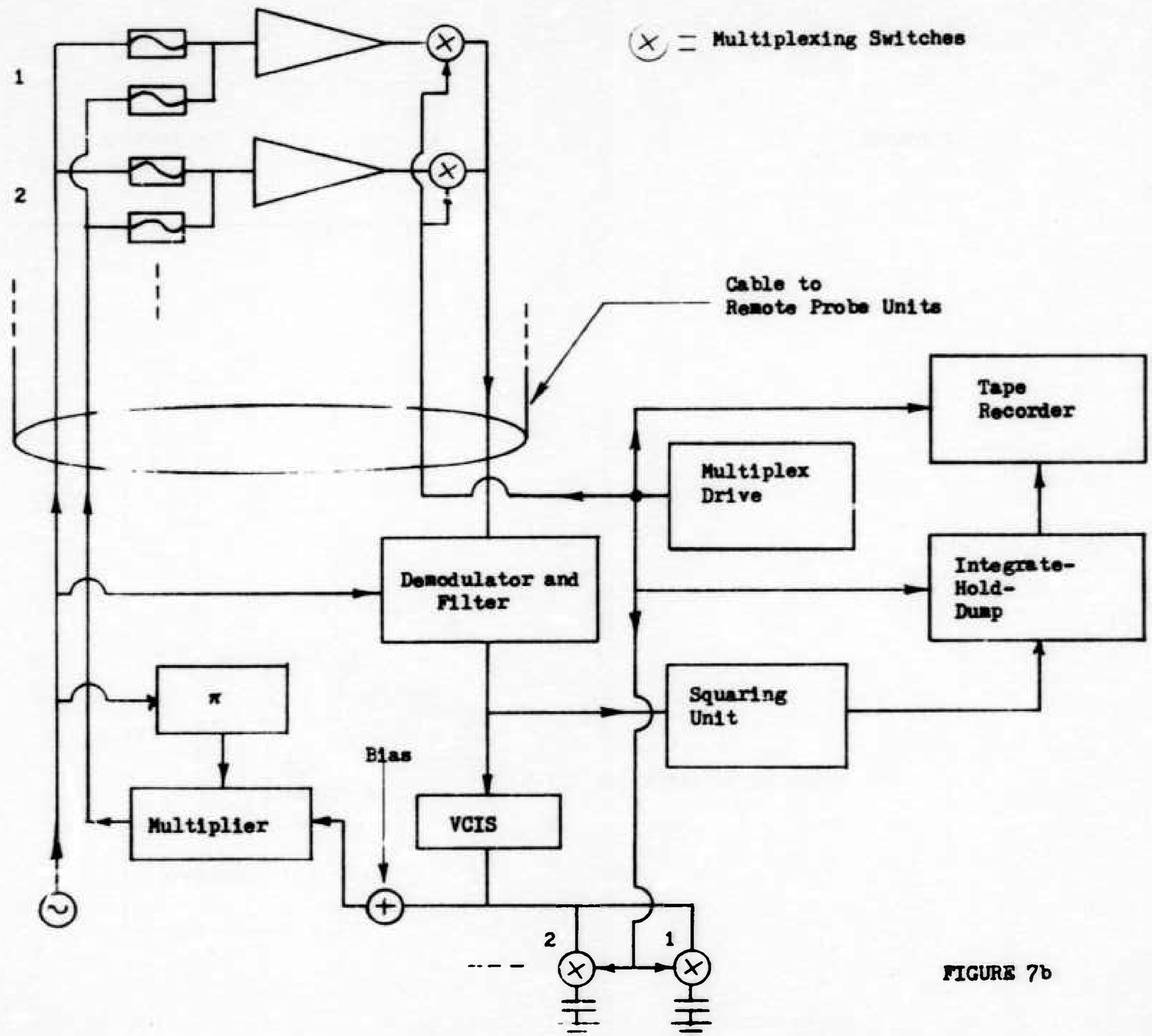
= Multiplexing Switches
1
2
Cable to
Remote Probe Units
Tape
Recorder
Multiplex
Drive
Integrate-
Hold-
Dump
Demodulator and
Filter
π
Squaring
Unit
Bias
Multiplier
VCIS
2
1

FIGURE 7b

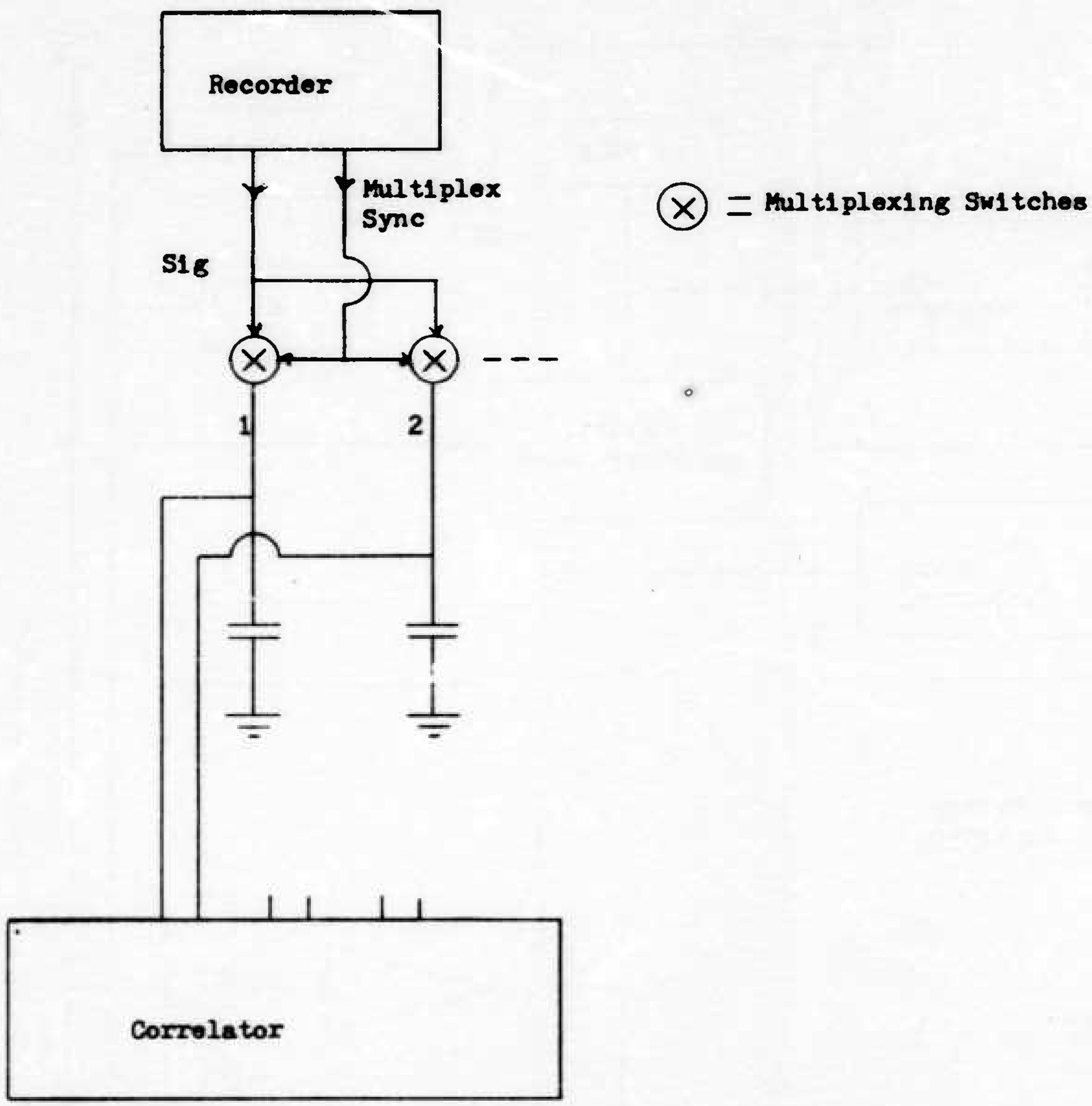

Recorder
Multiplex
Sync
Sig
1
2
Correlator
= Multiplexing Switches

FIGURE 8

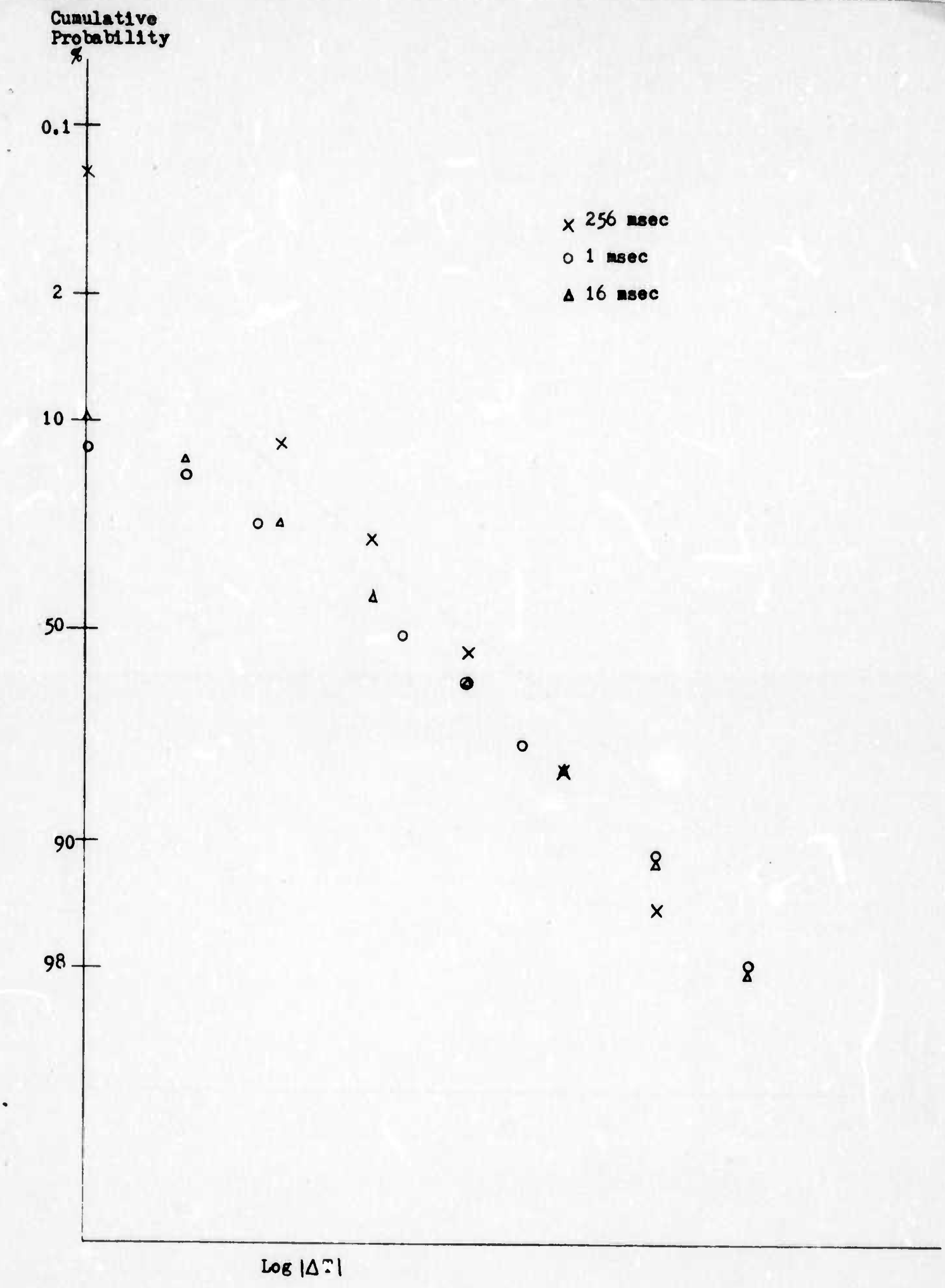
Cumulative Probability %
0.1
2
10
50
90
98
× 256 msec
o 1 msec
Δ 16 msec
Log |ΔT|

FIGURE 9a

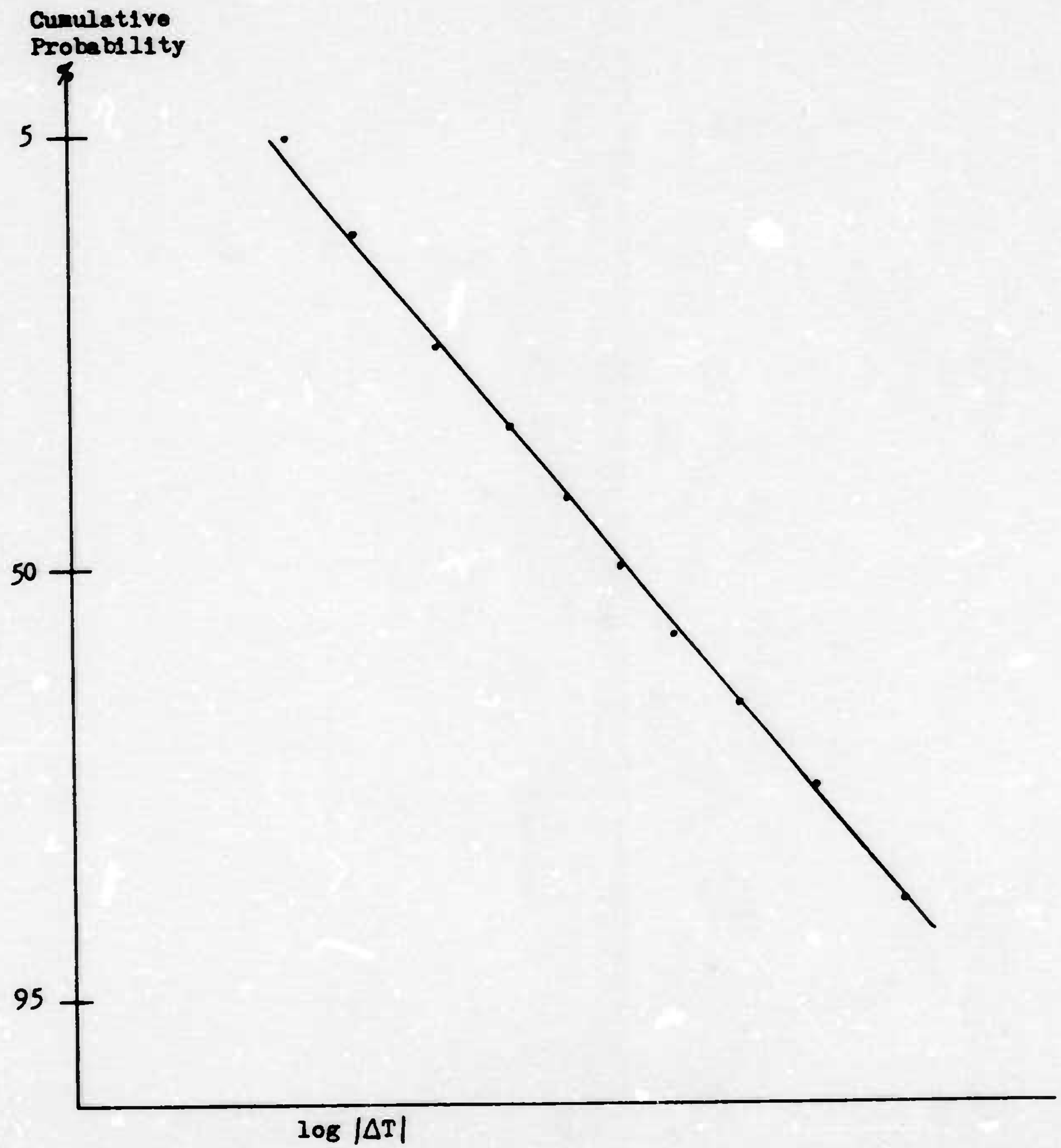

FIGURE 9b

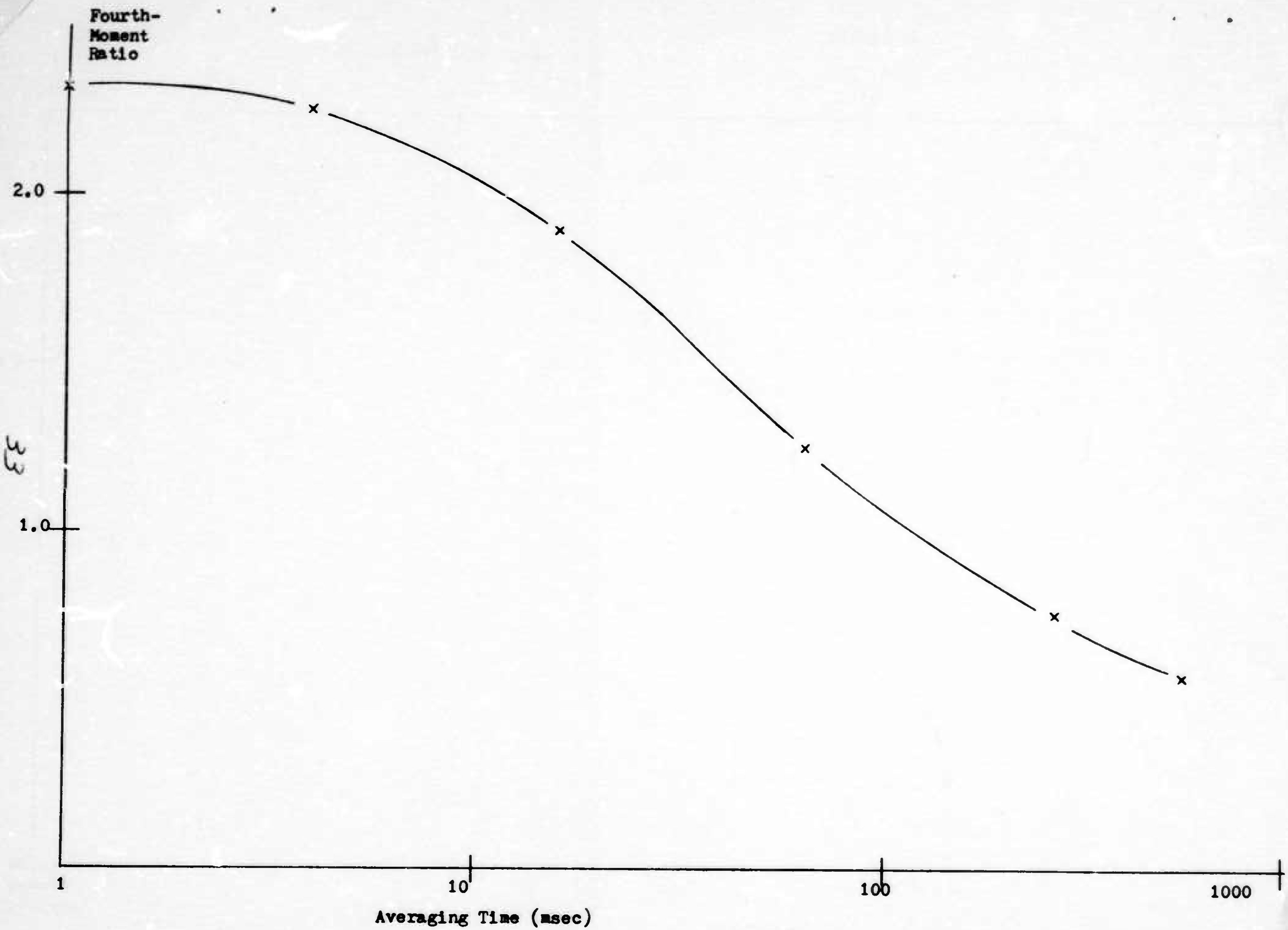

FIGURE 10

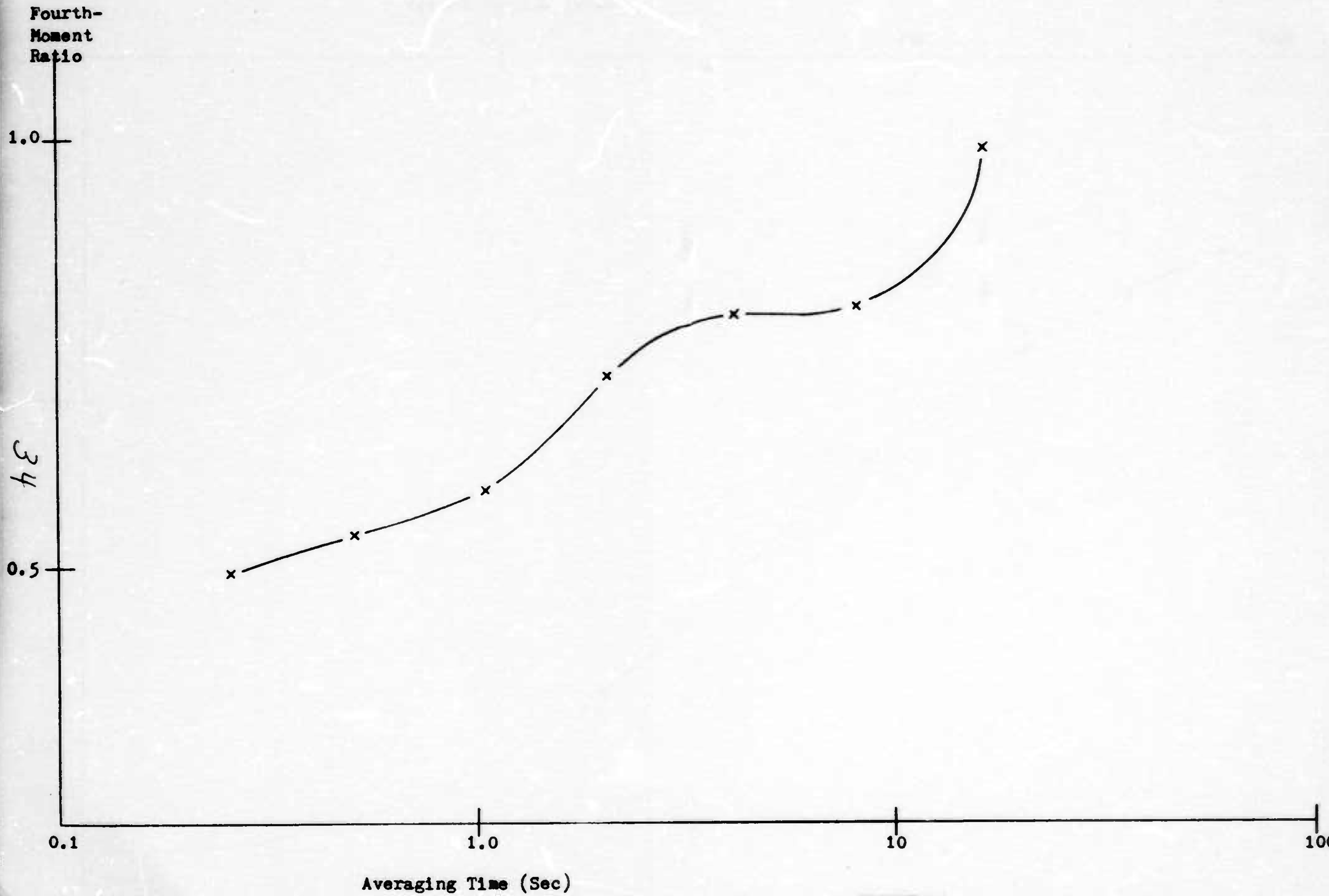

FIGURE 11

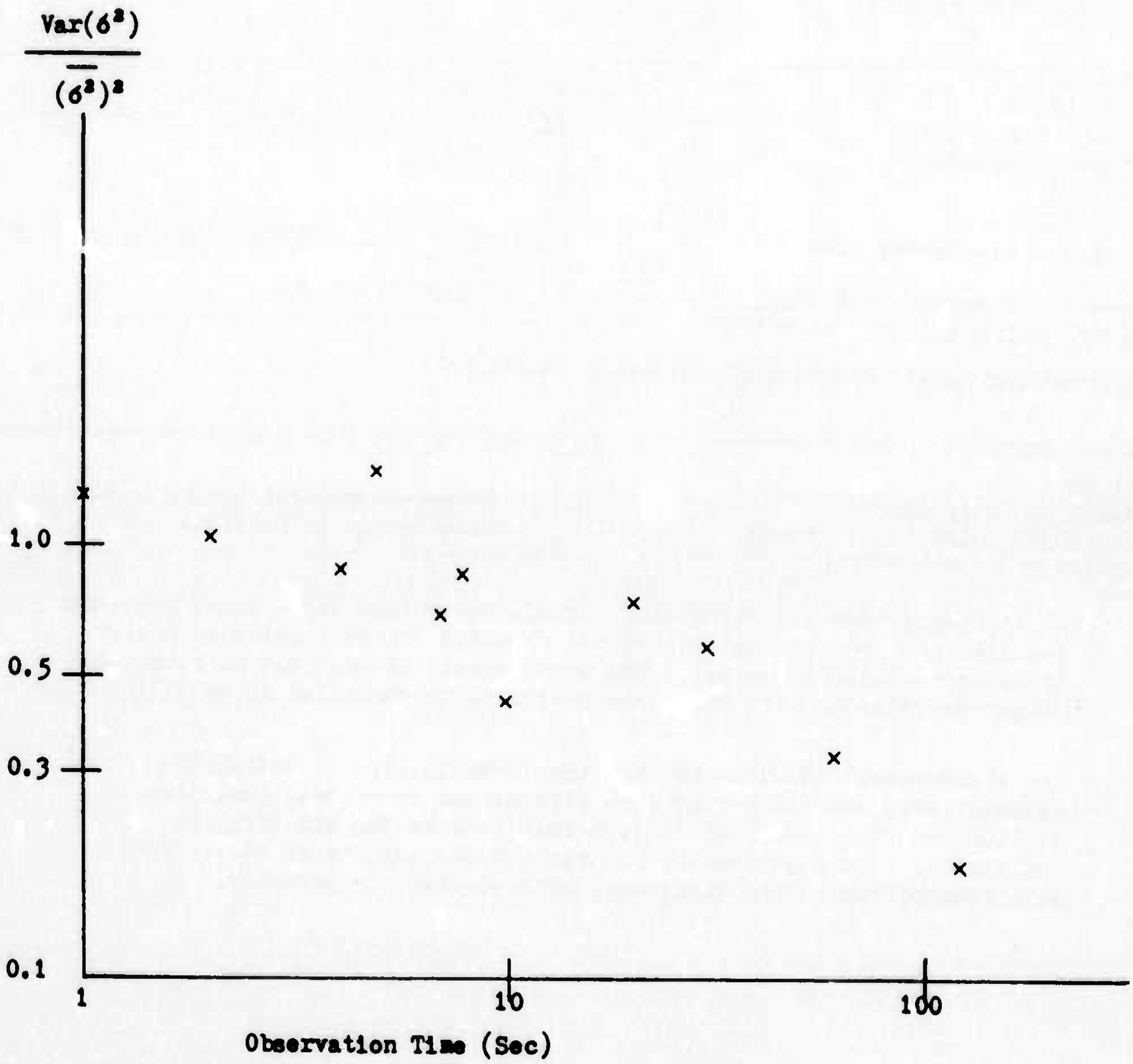
$\frac{Var(\sigma^2)}{(\overline{\sigma^2})^2}$
1.0
0.5
0.3
0.1
1
10
100
Observation Time (Sec)

FIGURE 12